The Core Metal-Recognition Domain of MerR†

Qiandong Zeng,[§,||] Christina Stålhandske,[⊥,#] Meredith C. Anderson,[⊥] Robert A. Scott,[⊥] and Anne O. Summers*[,§]

The Departments of Microbiology and Chemistry, University of Georgia, Athens, Georgia 30602

Received July 21, 1998; Revised Manuscript Received September 3, 1998

ABSTRACT: MerR, the metalloregulatory protein of the mercury-resistance operon (*mer*) has unusually high affinity and specificity for ionic mercury, Hg(II). Prior genetic and biochemical evidence suggested that the protein has a structure consisting of an N-terminal DNA binding domain, a C-terminal Hg(II)-binding domain, and an intervening region involved with communication between these two domains. We have characterized a series of MerR deletion mutants and found that as little as 30% of the protein (residues 80−128) forms a stable dimer and retains high affinity for Hg(II). Biophysical measures indicate that this minimal Hg(II)-binding domain assumes the structural characteristics of the wild-type full-length protein both in the Hg(II) center itself and in an immediately adjacent helical protein domain. Our observations are consistent with the core Hg(II)-binding domain of the MerR dimer being constituted by a pair of antiparallel helices (possibly in a coiled-coil conformation) comprised of residues cysteine 82 through cysteine 117 from each monomer followed by a flexible loop through residue cysteine 126. These antiparallel helices would have a potential Hg(II)-binding site at each end. However, just as in the full-length protein, only one of these potential binding sites in the deleted proteins actually binds Hg(II).

The bacterial mercury resistance (*mer*) locus carried by the transposable element Tn*21* consists of five structural genes, *merTPCAD*, involved in reducing reactive ionic mercury, Hg(II), to volatile, mercury vapor, Hg(0) (*1*), thereby removing this toxic metal from the bacterium's environment. This operon is controlled at the level of transcriptional initiation by a Hg(II)-responsive regulatory protein, MerR, whose own promoter overlaps partially with that of the structural genes, but is transcribed divergently (*2*). MerR actively represses structural gene transcription in the absence of Hg(II), activates expression of this transcript when Hg(II) is present, and also represses its own transcription, whether Hg(II) is present or not. The protein carries out all of these processes while bound to a single position on the DNA (the *mer* operator DNA, MerO), which lies between the −10 and the −35 RNA polymerase recognition hexamers of the promoter for the structural genes (P_{TPCAD}). One novel feature of MerR-mediated regulation (*3*−*5*) is that, even in the absence of Hg(II), it sequesters σ^{70} RNA polymerase holoenzyme at P_{TPCAD} in a nontranscribing condition called "active repression" (*6*, *7*). Hg(II) binding to DNA-bound MerR results in an allosteric transition in the protein (ref *8* and R. Kulkarni, unpublished observations) and a subsequent underwinding of the operator DNA which facilitates open complex formation at P_{TPCAD} (*9*−*11*).

Prior genetic and biochemical observations (*12*−*18*) suggest that the 144 amino acid residues of MerR form three functional domains: an N-terminal DNA-binding domain, a C-terminal Hg-binding domain, and an intervening region which plays a role in active repression and in transcriptional activation possibly by communicating the occupancy state of the Hg(II)-binding domain to the DNA-binding domain. The DNA-binding domain is characterized by a predicted helix−turn−helix motif (residues L8 through R29), whose affinity for MerO can be destroyed by a single E22K mutation in the second helix (the putative "recognition helix") (*12*). The MerR Hg(II)-binding domain has three conserved cysteine residues at positions C82, C117, and C126, which form a trigonal Hg(II) coordination site involving C117 and C126 from one monomer and C82 from the other (*17*−*22*). Thus, the high-affinity, high-specificity metal-binding site of MerR bears no obvious resemblance to known intrapolypeptide−chain metal sites characteristic of the myriad variations on the Zn-finger motif or the iron−sulfur centers of redox proteins. MerR activates transcription in vivo and in vitro with an apparent affinity of 10^{-8} M for Hg(II) in the presence of millimolar thiols (*10*, *23*); a similar response to other Group 12 (Zn, Cd) and noble (Au, Ag) metals requires 100- to 1000-fold higher concentrations of these metals than of Hg(II) (*23*). Purified MerR binds Hg(II) with a $K_{0.5}$ of 10^{-7} M in 10 mM β-mercaptoethanol (BME) and it does not bind Zn(II) detectably under the same conditions (*13*). The in vitro affinity of MerR for other metals has not been examined. Despite the fact that to date all in vitro studies with purified MerR protein show only a single Hg(II) ion bound per dimer with high affinity, with both in vivo transcriptional fusions and in vitro transcription assays, the MerR-mediated response to metal induction is hypersensitive, with a Hill coefficient of 2−3 (*10*, *23*). The mechanistic

† This work was supported by NIH grant GM28211 to A.O.S., GM42025 to R.A.S., and an NSF-RTG Center for Metalloenzyme Studies traineeship to M.C.A.

* Correspondence should be addressed to this author. Telephone: (706) 542-2669. Fax: (706) 542-6140. E-mail: summers@arches.uga.edu.

§ Department of Microbiology.

⊥ Department of Chemistry.

|| Present address: Genome Therapeutics Corporation,Waltham, MA.

Present address: University of Uppsala, Uppsala, Sweden.

10.1021/bi9817562 CCC: $15.00
Published on Web 10/23/1998

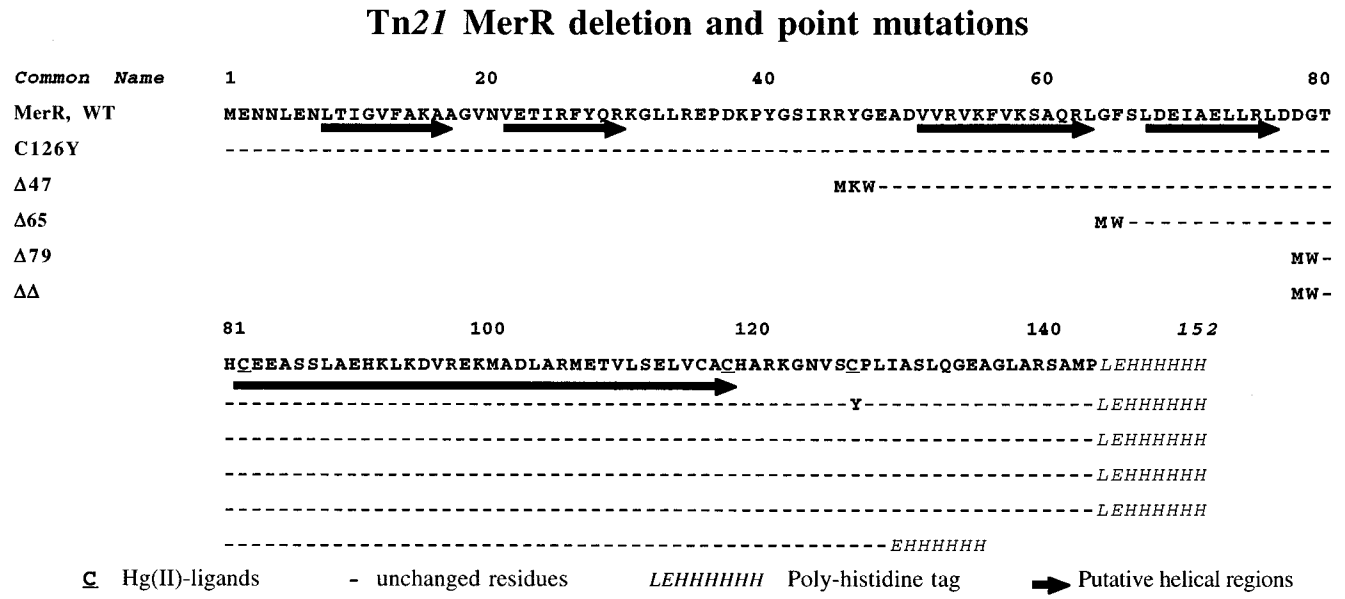

FIGURE 1: Tn*21* MerR wild-type, deletion, and point mutants. The top line is the wild-type amino acid sequence in standard single-letter abbreviation. The cysteine residues (C) are Hg(II) ligands. In subsequent lines, dashes indicate residues identical to the wild-type and substitutions are indicated as appropriate in single-letter code. Italics indicate the polyhistidine tag. Arrows indicate regions of predicted helical structure.

basis of this apparent cooperativity has not been determined.

The chemical basis of the striking affinity and specificity of MerR for Hg(II) may lie in its unusual trigonal cysteine coordination of the mercuric ion (*24*−*26*). We expect that there are functional elements of the protein, beyond the cysteines themselves, which serve to establish the propensity of these key residues for high-affinity Hg(II)-binding and also communicate the occupancy of the metal-binding site to the DNA binding site. To test this expectation, we constructed a series of N- and C-terminal deletion variants of the protein encoded by *merR* from transposon Tn*21*, and characterized their interactions with Hg(II) by several biochemical and biophysical methods. Our observations led us to conclude that as little as one-third of MerR (residues from Cys80 to Cys128)[1] is sufficient to form a single stable, dimeric, trigonally coordinate, high affinity Hg(II)-binding site.

EXPERIMENTAL PROCEDURES

Bacterial Strains and Plasmids. Plasmid pWR2 from *E. coli* strain CAG1574(pWR2) [*ara*D139 Δ(*ara leu*)*7697* Δ*lacX74 galU galK hsdR rpsL recA56 srl /ApR*] (*27*) was used for polymerase chain reaction (PCR) cloning of the *merR* wild-type and deletion mutants. Plasmid pWR217 from *E. coli* strain CAG1574(pWR217) [*araD139* Δ*(ara-leu)7697* Δ*lacX74 galU galK hsdR rpsL recA56srl /ApR*] (*27*) was used for PCR amplification of the C126Y mutant. Plasmid pET-21b(+)(*ApR*) (Novagen, Madison,WI) was used for cloning and expression of *merR* wild-type and mutants. *E. coli* strains DH5α [*lac*Δ*U169 Ø80lacZ*Δ*M15 thi-1 supE44 recA1 hsdR17 endA1 gryA96 relA1*] and BL21(DE3) [F^-*ompT hsdS*$_B$*(*rB^- *MB*$^-$*) lon gal dcm l(DE3)*] were used for mutant cloning and colony screening, and for protein expression, respectively. *E. coli* strains SK1592(pDU202) (*gal thi øRT1 sbcB15 endA/ aadA1 cat sul mer*) and J53(pPB1139) (*pro22 met63 nalR /aadA1 cat sul merR::Tn5*) (*28*) were used for genetic complementation tests.

Construction of His-Tagged MerR Derivatives. The DNA amplicands for expression of MerR wild-type and mutant proteins were generated by PCR and cloned into the vector pET-21b(+) (Novagen) between *Nde*I and *Xho*I sites, for expression of C-terminal hexahistidine tagged full-length MerR and deletion or point mutation proteins (Figure 1). For wild-type and deletion mutants, the PCR template was the *Bam*HI-linearized plasmid pWR2 from strain CAG1574 (pWR2) and the PCR template for C126Y was CAG1574-(pWR217)(*27*). Each of the N-terminal deletion derivatives is named according to the position of the last residue removed, e.g., the first native residue in the mutant Δ47 is residue 48. Since MerR contains no Trp and even the shortest of the deletions removes all of the Tyr residues in the protein, a single Trp residue was added immediately after the initiating Met to each of the mutant proteins to facilitate quantification by absorbance at 280 nm. An additional Lys residue was also incorporated in Δ47 in order to avoid a potential hairpin in the primer. The N-proximal leucine was not included in the His-tag for the N- and C-terminal deletion derivative, ΔΔ, because the native residue immediately preceding the His-tag is Leucine 128. The PCR primers used for the construction of deletion mutants include: 5′-TCAC-TACACATATGGAAAATAATTTGGAAAACC-3′ (primer 1) and 5′-AATACTCGAGAGGCATAGCTGACCTTG-3′ (primer 2; for wild-type and C126Y), 5′-TAAATACATAT-GAAATGGGCGGACGTGGTTCGGG-3′ (primer 3; with primer 2, for Δ47), 5′-TATTATCATATGTGGAGTCTG-GACGAGATTGCCG-3′ (primer 4; with primer 2, for Δ65), 5′-TATAATCATATGTGGACCCACTGCGAGGAGGC-3′ (primer 5; with primer 2, for Δ79), 5′-AATACTC-

[1] Abbreviations: BME, β-mercaptoethanol; BSA, bovine serum albumin; DTT, dithiothreitol; Cys or C, cysteine; ESI-MS, electrospray ionization mass spectrometry; EXAFS, extended X-ray absorption fine structure; FPLC, fast protein liquid chromatography; HPLC, high-pressure liquid chromatography; PMSF, phenyl methylsulfonyl fluoride; XAS, X-ray absorption spectroscopy.

GAGCGGGCAGGAAACATTC-3′ (primer 6; with primer 5, for ΔΔ which removes N-terminal residues 2−79 and C-terminal residues 129−144). The *Nde*I (CATATG) and *Xho*I (CTCGAG) recognition site sequences are underlined. For insertion of the amplicands into the expression vector, we used the "near-zero-background" cloning method (*29*) which resulted in recoveries of 80−100% correct inserts in a single transformation step. The recombinant plasmids were purified using Qiagen Plasmid Midi-Prep (Qiagen, Chatsworth, CA), and the inserts were verified by sequencing of both strands at the University of Georgia Molecular Genetics Instrument Facility. All proteins used in this study were His-tagged; for simplicity this term will not be included in their names every time they are mentioned.

Complementation by His-Tagged Full-Length Wild-Type MerR. Strains SK1592 (pDU202) with the wildtype *mer* operon and J53(pPB1139) with a *mer* operon carrying the defective *merR::*Tn*5* allele (*28*) were mated on tryptone plates with BL21(DE3)(pQZMerR-H6) encoding the full-length, wild-type MerR protein with the C-terminal His-tag or with BL21(DE3)(pET21-b(+)) carrying the vector alone. Exconjugants were selected on tryptone agar plates containing chloramphenicol (Cm), 20 μg/mL, and ampicillin (Ap), 100 μg/mL. Several exconjugant colonies from each cross and the corresponding Hg(II)-resistant or -sensitive control strains were streaked on tryptone agar containing relevant selective antibiotics and 50 μM Hg(II) with or without 100 μM isopropylthiogalactoside (IPTG) for induction of MerR expression. After overnight incubation at 37 °C, formation of isolated colonies indicated Hg(II) resistance.

Protein Expression and Purification. BL21(DE3) strains carrying wild-type or mutant clones were grown at 37 °C to $OD_{600} = 0.6$, and induced with 100 μM IPTG for 1.5 h, with the exception of double deletion mutant, ΔΔ, whose protein yield was better when grown at 25 °C and induced with 100 μM IPTG for 5 h. Cells were harvested at 4 °C by centrifugation at 5000*g* for 10−15 min. The pellet was suspended in 20 mM Tris, pH 7.9, 0.5 M NaCl, 0.6 mM PMSF, and 1 μg/mL leupeptin. The cells were broken by four passes through a French Pressure cell at 17 000 psi. After centrifugation at 35000*g* for 2.5 h, the cytosol from ∼5 g of wet cells was passed through a 0.2-μm filter and loaded onto a column of 2.0 mL of Ni(II)-His·Bind resin (Novagen, Madison, WI) which had been prewashed with 10 mL of binding buffer (5 mM imidazole, 20 mM Tris-HCl, pH 7.9, 0.5 M NaCl). After sample was loaded, the column was washed with 30 mL of binding buffer, followed by 30 mL of wash buffer (60 mM imidazole, 0.5M NaCl, 20mM Tris-HCl, pH 7.9). The His-tagged protein was eluted from the column with 15 mL of argon-purged strip buffer (100 mM EDTA, 0.5 M NaCl, 20 mM Tris-HCl, pH 7.9, 10% glycerol, and 10 mM BME; BME was added after argon purge and immediately before use). The eluted His-tagged protein was concentrated in an Amicon cell with a YM10 membrane (molecular weight cutoff 10 kDa) and exchanged into argon-purged buffer 1 (0.5 M NaCl, 10% glycerol, 50 mM Tris-HCl, and 10 mM BME, added immediately before use). The preparations were concentrated to ∼2−6 mg of protein/mL in a 3−5 mL final volume and stored at −70 °C. Purified His-tagged MerR was free of any of 30 metals (including Ni, Zn, Au, Ag, and Hg) as assessed by inductively coupled plasma atomic absorbance carried out at the University of Georgia Chemical Analysis Laboratory.

Protein Quantification. Protein concentrations for wild-type full-length MerR were calculated on the basis of its molar extinction coefficient at 280 nm (4080 M^{-1} cm^{-1}) predicted from its composition (3 Tyr, 4 Cys, no Trp) (*30*) and agreed well with concentrations determined by the Bradford reagent using bovine serum albumin (BSA) as a standard. The protein concentrations for the deletion mutants were calculated on the basis of the molar extinction coefficients of the single Trp and the 4 Cys at 280 nm (5930 M^{-1} cm^{-1}). The extinction coefficients at 280 nm for the smaller deletion derivatives did not correlate as well with the BSA-standardized Bradford assay as did the full-length proteins. Thus, correction factors of between 1.07 and 1.78 (depending on the mutant) were determined for use when the Bradford assay was required for quantification of small amounts of protein.

DNA Binding. The gel shift protocol of Heltzel et al. (*31*) was followed with some modifications. Each protein was mixed (at 2−9 μM final concentration) with 225-bp PCR amplicand (at 2−5 μM final concentration) containing the Tn*21 mer* operator/promoter (MerOP) and incubated on ice for 30 min. The binding buffer contained 12 mM HEPES, 12% glycerol, 1mM EDTA, 5 mM $MgCl_2$, 60 mM KCl, 0.6 mM DTT (added freshly), and 0.2 mg/mL BSA. The 20-μL reaction was mixed with 2 μL of loading dye (0.1% bromophenol blue and 50% glycerol) and loaded onto an 8% acrylamide/bis-acrylamide gel for electrophoretic separation at 80 V for ∼2 h. After ethidium bromide staining, the gel was scanned with a Molecular Dynamics Fluoroimager and relative band intensities were compared using the ImageQuant software (Molecular Dynamics, Sunnyvale, CA).

Mass Spectrometry. To determine the molecular mass of the overexpressed proteins and to make initial assessments of their dimerization and Hg(II)-binding properties two conditions were used for mass spectrometry:

a. Coupled HPLC electrospray ionization mass spectrometry (HPLC-ESI-MS) was used for all proteins. The proteins in buffer 1 [with or without a 5-fold molar excess of Hg(II)] were reacted for 60 min on ice and then subjected to reversed-phase liquid chromatography on a micropore C4 column (mobile phase acetonitrile/water gradient with 0.01% trifluoroacetic acid) coupled with electrospray mass spectrometry (Perkin-Elmer Sci-Ex APII Plus).

b. Direct electrospray ionization mass spectrometry (ESI-MS) was used only with wild-type MerR. Protein (50−250 μg) was exchanged from buffer 1 with or without BME [and with or without 2 or 3 molar excess of Hg(II)] into 0.1 M acetic acid or ammonium acetate by five repeated concentrations and dilutions in a Microcon concentrator (Amicon, Inc., Beverley, MA). Samples, in either acetic acid or ammonium acetate, were directly injected into the ESI-MS (Perkin-Elmer Sci-Ex APII Plus).

Circular Dichroism (CD). CD spectra were recorded at room temperature with 5.0 μM (dimer) protein solution in buffer 1 with freshly added BME using a 1-mm lightpath CD cell in a Jasco J-715 spectrometer (Jasco, Inc., Easton, MD). At least five scans were recorded and averaged for each experimental condition and the data were reduced using the Jasco software. The lower limit of usable data was ∼200 nm, owing to the high absorbance at lower wavelengths of the 10 mM BME used in all buffers.

Gel Filtration Chromatography. The monomer−dimer distributions for the full-length MerR wild-type and the most extensively deleted variant, ΔΔ, were determined by gel filtration on a Progel-TSK QC-PAK GFC200 column (15 cm × 7.8 mm i.d., particle size 5 μm, pore size 125 Å) (Supelco, Bellefonte, PA) run on a Pharmacia LC501 Plus FPLC system with an LKB UV-MII monitor. The mobile phase was argon-purged buffer 1, prepared by purging buffer 1 (minus BME) with argon for 3 h and storing it in an anaerobic Coy chamber (Coy Laboratory Products, Inc., Grass Lake, MI) until use. Immediately before use, BME was added to the buffer at a final concentration of 10 mM. The buffer reservoir was then removed from the Coy chamber, attached to the FPLC mobile phase inlet, and sealed with Parafilm. MerR protein samples were diluted into argon-purged buffer 1 in the Coy chamber, and immediately after removal from the Coy chamber, were injected in 50-μL aliquots (via a 50-μL loop) onto the column. The buffer flow rate was 0.9 mL/min and protein absorbance was monitored at 280 nm. The column was calibrated with the following molecular weight standards (from Sigma, Inc.): bovine lung aprotinin (6500 Da), horse heart cytochrome *c* (12 400 Da), myoglobin (17 000 Da), bovine carbonic anhydrase (29 000 Da), ovalbumin (44 000 Da), and bovine serum albumin (66 000 Da). All sample conditions were run at least in triplicate and were reproducible.

Hg(II) Binding. a. Equilibrium Ultrafiltration. The relative affinity for Hg(II) of MerR wild type and its variants was examined by ultrafiltration (*32*). MerR protein (in concentrations ranging from 1 to 10 μM as the dimer) was mixed with $HgNO_3$ in a total volume of 1.0 mL of buffer 1 resulting in $Hg/MerR_2$ ratios from 0.2 to 10. After incubation on ice for 1 h, each mixture was transferred to the upper chamber of a Millipore Ultrafree MC unit (MWCO 5000 Da, capacity 2 mL), and centrifuged in a Beckman JA-17 rotor at 5000*g* for exactly 7.5 min at 4 °C to achieve a 60−80 μL spin-through volume in the lower chamber of each unit. The Hg(II) concentrations of the resulting solutions in the upper and the lower chambers of the ultrafiltration units were determined by wet-ashing using a Leeman Autodigestor AP200, followed by quantification of total Hg using cold vapor atomic absorption spectroscopy on the Leeman PS200II (Leeman Labs, Inc., Lowell, MA). Total Hg(II) recovered from the upper and lower compartments was typically ∼90%. Protein content of both compartments was determined using the Bradford reagent with BSA as a standard. No penetration of protein to the lower chamber was noted for any variant. The total protein recovered in the upper chambers was typically 78−95% of the starting amount, owing to some tendency of MerR to stick to surfaces. Stoichiometry of Hg(II) binding was calculated using the actual soluble protein in each upper chamber and the actual Hg assayed in the upper and the lower chambers.

b. Nonequilibrium Dialysis. MerR proteins (10 μM dimer) were incubated in argon-purged buffer 1 containing 50 μM $HgNO_3$ for 1 h at 4 °C. Then 0.8 mL of each reaction was transferred into a screw-capped DispoDialyser tube (1.0 mL capacity, 8000 Da MWCO, Spectrum, Houston, TX) and dialyzed against 1 L of stirred, argon-purged buffer 1 for 1 h at 4 °C. The tubes were then transferred to 1 L of fresh argon-purged buffer 1 and dialyzed for an additional 20 h at 4 °C. The total Hg concentration in each dialysis tube was monitored by periodic sampling. A dialysis tube containing the same initial concentration of Hg(II) but no protein was used to determine the rate of free diffusion of Hg(II); 90% of the Hg(II) had left this tube within the first hour of dialysis. The protein concentration in each tube was determined for the initial and final samples; slight losses of the two smallest proteins from the dialysis bags were noted and the corresponding Hg(II) diffusion rates (nanomoles of Hg lost/hr per mole of protein) were corrected accordingly.

Table 1: EXAFS Data Collection Conditions

SR facility	SSRL
beamline	7-3
monochromator crystal	Si[220]
detection method	fluorescence
detector type	13-element solid-state array
scan length (min)	20−22
scans in average	8−18
metal concentration (mM)	0.2−0.7
temperature (K)	10
energy standard	Hg/Sn amalgam foil (first inflection)
energy calibration (eV)	12 285
E_0 (eV)	12 295
pre-edge background energy range (eV) (polynomial order)	11 960−12 250 (−1)
spline background energy range (eV) (polynomial order)	12 295.0−12 559.5 (4) 12 559.5−12 824.0 (4) 12 824.0−13 088.5 (4)

X-ray Absorption Spectroscopy (XAS). MerR and mutant proteins were mixed with a 4-fold molar excess of Hg(II) in buffer 1 (total volume ∼2.0 mL), dialyzed in a 3.0 mL Slide-A-Lyzer (10 000 Da molecular weight cutoff, Pierce, IL) against 1.2 L argon-purged buffer 2 (0.5M NaCl, 10% glycerol, 10 mM Tris-HCl, pH 7.9, and fresh 10 mM BME) for 5.0 h with three changes of buffer, and concentrated to ∼100 μL in a 3-mL Centricon-10 (Amicon) by centrifugation at 4 °C. The samples were adjusted to ∼30−40% glycerol, loaded into XAS cuvettes, and quick-frozen in liquid nitrogen. For anaerobic preparations, all steps except the centrifugation were performed either in a Coy anaerobic chamber or a Plas-Labs, Inc. (Lansing, MI) gloveless anaerobic chamber. XAS data were collected on protein solutions containing from 0.2 to 4 mM MerR-Hg(II) at the Stanford Synchrotron Radiation Laboratory (SSRL) beamline 7-3, with SPEAR ring operating at 3.0 GeV and between 50 and 100 mA. Table 1 describes the data collection conditions and data reduction parameters. Curve-fitting analysis of the EXAFS data was performed using the EXAFSPAK software packaged developed by G. N. George (SSRL; http://ssrl01.slac.stanford.edu/exafspak.html) with theoretical scattering parameters.

Secondary Structure Prediction and 3D Structure Modeling. The secondary structure of MerR was predicted on the consensus of 10 different algorithms including the GOR method and the Chou-Fasman method (Wisconsin Genetics Computer Group, Inc). The SSPRED method was available from http://www.embl-heidelberg.de/sspred/sspred_info.html (*33*) and the remaining seven methods were available via WWW-based sequence analysis services (http://www.ibcp.fr/serv_pred.html and http://www.embl-heidelberg.de/predictprotein/ppHelp.html) (*34*). The N-terminal residues of the helix-turn-helix DNA binding motif were assigned according to Brennan et al. (*35*). Prediction of the propensity

to form coiled-coil structures was made using the programs MultiCoil (*36*) and COILS (*37*). The potential for structural similarity of MerR residues Cys82 through Cys117 to other coiled-coil proteins was assessed using the threading algorithm available from EMBL-Heidelberg (*34*).

RESULTS

The Design of the MerR Deletion Mutants. Secondary structure predictions strongly suggested that MerR has a highly α-helical content distributed in five distinct segments separated by less structured regions (Figure 1). The first two predicted helices (L8-A18 and V21-R29) would form a helix−turn−helix motif (*35*) and the latter of these two predicted helices is definitely implicated in DNA binding (*13*, *27*). This putative "recognition helix" is followed by a predicted loop from residues 44 through 47, a region which may be solvent-exposed because the corresponding region in the MerR protein from *Bacillus* strain RC607 is protease sensitive (*8*). The next two predicted helices are V51-L63 and L67-L76 and mutants in these regions affect activation and/or repression but are unimpaired in Hg(II) binding (*13*, *18*, *27*). The last predicted α-helical region is the longest and most strongly predicted (by all algorithms); it would stretch from residues C82 through C117, a distance of ∼55 Å if in a standard α-helical fold. A subset of this region is also predicted to assume either a parallel or an antiparallel coiled-coil structure (*36*, *37*) and to be capable of forming a structure similar to the coiled-coil regions of proteins such as spectrin, Jun, and Fos (*34*). In the chromosomal homologue of MerR, YhdM (*38*), the corresponding region is even more strongly predicted to assume a coiled-coil conformation, than in MerR. [The actual function of YhdM is not known but it may regulate metal ion transport, possibly via the recently described Zn(II) efflux protein, ZntA (*39*).] The region beyond C117 in MerR is predicted to be without regular structure and the observation of a trypsin-sensitive site around residue 120 or 121 in Tn*501* MerR (*13*) suggests this region may be solvent-exposed as well.

On the basis of the foregoing analysis, we designed four mutants deleted for varying extents from the N-terminus of MerR (Figure 1). The least extensive deletion mutant, Δ47, removed the first two helices which constitute the putative DNA-binding domain. The deletion end-points of the next two mutants, Δ65 and Δ79, were designed to occur within predicted loop regions and they extended through the third and the fourth helices, respectively. The most extensive deletion, ΔΔ, removed residues from 2 through 79 (including all four putative N-terminal helices) and also from 129 through 144 and was designed to achieve a minimal Hg(II)-binding domain. The histidine affinity tag was placed at the C-terminus of each derivative because this is the least conserved region of the protein (*40*) and because random replacement or removal of the last 15−17 residues at the MerR C-terminus does not affect the response of MerR to inorganic Hg(II) (*41*, *42*). Initial observations (see below) indicated that the His-tagged derivative of wild-type MerR retained the expected in vivo and in vitro functions. Thus, to minimize the number of non-native residues added, a protease recognition site was not included in the junction between the native MerR sequence and the His tag in any of the derivatives. Since all of the MerR deletion mutants have lost the three tyrosine residues of the full-length protein, a single tryptophan residue was placed in the +2 or +3 position at the N-terminus of each deletion mutant to facilitate protein quantification by absorbance at 280 nm.

A point mutation in *merR* (resulting in the change C126Y) (*27*) was used as a control in these experiments as its impaired Hg(II) binding has been previously described. This protein has an apparent affinity for Hg(II) of only ∼25% of that of the wild-type MerR (*13*) and is completely nonresponsive to Hg(II) in vivo (*27*).

In Vivo and In Vitro Function of the His-Tagged MerR Proteins. To discover whether addition of the affinity tag had any deleterious effect on the in vivo functioning of wild-type MerR, the His-tagged derivative of wild-type full-length MerR was tested for its ability to complement a *merR::Tn5* insertion in the Tn*21 mer* operon (carried on the conjugative plasmid pDU202) for expression of Hg(II) resistance. The His-tagged MerR complemented the defective *merR* of pPB1139 (*28*) in *E. coli* strain J53, allowing the strain to form isolated colonies on 50 μM $HgCl_2$-supplemented medium. The vector pET-21b(+) alone did not complement pPB1139. Thus, the His tag attached to the MerR C-terminus does not interfere with the protein's function in vivo. In gel shift assays, the full length, wild-type, His-tagged MerR quantitatively retarded the mobility of a 225 bp DNA fragment containing the *mer* operator−promoter at 1:1 MerR dimer/DNA molar ratio. By using the same conditions MerR-C126Y bound DNA indistinguishably from the full length wild-type MerR, and none of the deletant proteins bound DNA at all. His-tagged, wild-type, full-length MerR also bound one Hg(II) per dimer (see below) and can form a preinitiation complex with RNA polymerase in vitro, distort DNA when Hg(II) is added, and activate transcription of the structural genes while repressing transcription of its own gene (R. Kulkarni and A. O. Summers, submitted for publication).

Expression and Recovery of Wild-Type and Mutant MerR Proteins. Although these constructs could produce as much as 40% of the total cellular protein as the MerR derivative, MerR produced at such high intracellular concentrations was almost exclusively in inclusion bodies. To avoid the ambiguities associated with renaturation of a sulfhydryl-rich protein lacking a facile assay, we adjusted the induction conditions to achieve expression of the MerR variants at between 5 and 10% of total protein. This resulted in ∼70−80% of the expressed proteins being soluble. However, at 37 °C the shortest derivative, ΔΔ, was produced as <1% of total cellular protein, so the growth temperature was reduced to 25 °C. This resulted in synthesis of ΔΔ at 3−5% of the total cellular protein, 70−80% of which was soluble. The typical yield from 1 L of cell culture for each of the derivatives ranged from 2 to 5 mg of purified protein. After affinity purification on Ni(II) columns, each protein preparation was at least 98% pure as determined by SDS-PAGE.

Electrospray Mass Spectrometric (ESI-MS) Characterization of the MerR Variants. HPLC-ESI-MS confirmed the peptide masses to within ±3 amu of the calculated monomer molecular masses including the N-terminal methionine (data not shown). We also observed that from zero to three BME molecules per monomer were attached to each protein. The limited numbers of such attached BME molecules is not likely due to adventitious adherence during electrospray solvent evaporation, since the mobile phase did not contain thiols and the free thiols of the sample eluted from the

column 20−30 min before the eluting protein was directed to the ESI chamber. These observations suggest that in the absence of Hg(II), three cysteines per monomer were able to form stable disulfide bonds with BME under the conditions used for the ESI-MS preparation.

When the MerR variants were mixed in buffer 1 with a 5-fold molar excess of Hg(II) prior to HPLC-ESI-MS, peaks corresponding to one Hg(II) per MerR monomer (and from zero to three BMEs) were also detected, although the apoprotein peaks (again with varying numbers of BMEs) remained major species. Even in the presence of the 1000-fold molar excess of BME in buffer 1, Hg(II) binding to the mutant C126Y was detected in HPLC-ESI-MS, despite the fact that the affinity of C126Y for Hg(II) is only 25% that of the wild-type protein (ref *14*, and see below). This suggests that C126Y is not completely impaired with respect to Hg(II) binding since its metal recognition site still competes, albeit somewhat less effectively, with buffer thiols. [Note that both C82Y and C117Y were previously shown to bind 1.0 Hg(II)/dimer in the presence of excess BME (*14*) even though each is also missing one of the key cysteine ligands and is completely uninducible by Hg(II) in vivo (*27*).] Moreover, the observation that in HPLC-ESI-MS no protein monomer bound more than one Hg(II) also indicated that the His tag did not introduce a new Hg(II)-binding site on MerR or its variants.

Under the highly denaturing conditions of HPLC-ESI-MS, MerR dimers were never observed [with or without added Hg(II)]. This suggests that there were no disulfide bridges nor any MerR−Hg−MerR bridges formed between the monomers in buffer 1 which were stable to the conditions of HPLC-ESI-MS. However, disulfide bridges between BME and the protein apparently were stable to HPLC-ESI-MS conditions, suggesting that if disulfide bonds at least as stable as these had formed between the protein monomers we could have seen them.

In contrast, under the solvent-exchange conditions used to prepare the wild-type MerR protein for direct ESI-MS, dimers of MerR (but not higher aggregates) were detected when BME was absent from the ammonium acetate or acetic acid desalting buffer (data not shown). When BME was included in the desalting buffer, only monomers (with varying numbers of attached BMEs) were observed after buffer exchange. The inclusion of Hg(II) along with BME in the desalting buffer resulted in monomers with a single Hg(II) attached; when BME was not included, dimers with a single Hg(II) were observed.

Circular Dichroism. Full-length MerR exhibits CD minima at 208 and 220 nm, characteristic of a protein with extensive α-helical content (Figure 2). (Note that the peak at 190 nm, characteristic of α-helical structure, was generally not observable owing to interference in this region by the 10 mM BME in the buffer.) Although the amplitudes of the peaks at 208 and 220 nm decrease in each of the smaller derivatives, the α-helical characteristics of these spectra remained, indicating that even the shortest protein is capable of forming this secondary structure.

Dimerization. The dimer stability was examined in the two most extreme cases: full-length wild-type MerR (monomer MW 16 967 Da; Figure 3a) and the most extensively deleted derivative, ΔΔ (monomer molecular weight 6680 Da; Figure 3b). Since HPLC-ESI-MS experiments (see above) suggested that no disulfide dimer was formed in buffer 1, we did not expect the monomer/dimer equilibrium to be influenced by the formation of disulfide dimer. Nonetheless,

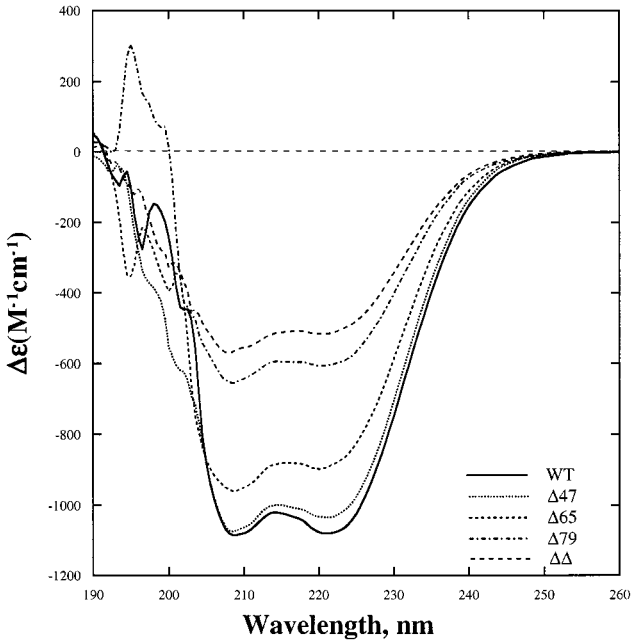

FIGURE 2: Far UV circular dichroism of MerR and its variants. The protein concentration was 5.0 μM (dimer) in buffer 1 (0.5 M NaCl, 10% glycerol, 10 mM BME, and 50 mM Tris-HCl, pH 7.9). Spectra were recorded at room temperature (25 °C) in 1-mm lightpath quartz cells. Symbols: wild-type, WT (solid line); Δ47, (···); Δ65 (- - -); Δ79 (-·-), ΔΔ (− − −).

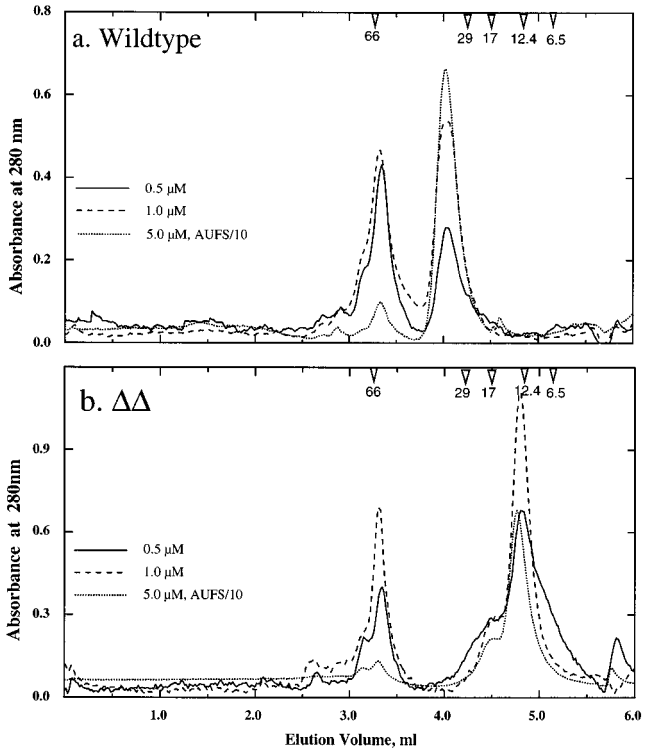

FIGURE 3: Gel filtration chromatography of MerR (a) wild-type and (b) mutant ΔΔ proteins. Arrows mark elution positions of protein molecular weight standards as listed in Experimental Procedures. Protein concentrations are indicated by the following symbols: 0.5 μM (solid line); 0.1 μM (- - -), 5.0 μM (···). The monomer molecular weights of MerR and of ΔΔ are 16 967 and 6680 Da, respectively.

we used argon-purged buffer and diluted the proteins into it in a Coy anaerobic chamber prior to loading onto the gel filtration column. At the 0.5 μM protein concentration or above, both full-length MerR and the $\Delta\Delta$ proteins dimerize almost completely, although protein trailing behind the ~13 360 Da $\Delta\Delta$ dimer peak (Figure 3b) suggested formation of some monomers at this lowest concentration. These observations indicate that dimerization was not significantly impaired even in the shortest derivative and, thus, residues C80 to C128 are sufficient to form a disulfide-independent dimer. The double deletion protein also produces a small trimer peak on the leading edge of the dimer peak at all concentrations and both proteins produced multimers of apparent molecular weight equal to or greater than 66 kDa eluting in the void volume (i.e., where BSA elutes from this column). Since this multimerization can take place even in the absence of Hg(II) and under highly reducing conditions, it may arise, as Fairman et al. have suggested for a model Lac repressor tetramerization domain (*43*), from the increased burial of hydrophobic surfaces in tetramers relative to dimers. Interestingly, at higher protein concentrations of both the full-length protein and $\Delta\Delta$ the relative proportion of dimer was greater than it was at lower concentrations.

X-ray Absorption Spectroscopy (XAS). The XAS data indicate that the full-length wild-type MerR and even its most extensively deleted variants have very similar Hg(II) environments (Figure 4A-B). The Fourier transform of the extended X-ray absorption fine structure (EXAFS) data for the full-length wild-type protein and the three N-terminal deletion derivatives (Figure 4A) indicates a single shell of scatters at about 2.40−2.44 Å, consistent with Hg in a HgS_3 site as seen previously (*20*). Indeed, the XAS data for the His-tagged Tn*21* MerR and its N-terminal deletion derivatives were indistinguishable from the observations made on Tn*501* MerR (*20*) (data not shown). Thus, even without its first 79 N-terminal residues, the remaining MerR protein can still assemble a Hg-binding site indistinguishable by EXAFS from that of the full-length protein.

The most extensively deleted variant $\Delta\Delta$ and the missense mutant C126Y bind Hg(II) less well (see below) than the full-length protein and the other deletion variants, making it difficult to achieve the high Hg concentrations for optimal XAS. However, despite the lower signal-to-noise ratio for these preparations, the EXAFS spectrum of the double deletion protein (Figure 4B) reveals that its Hg(II)-binding site is very similar to that of the full-length protein and to the HgS_3 model compound. Although our conclusions are tempered by the weak Hg signal available for the C126Y variant, its edge is more consistent with HgS_3 than with HgS_2, HgS_4, or HgO_1S_2. The EXAFS of C126Y (Figure 4 B) indicates that the Hg−S bond lengths are slightly longer than those of the wild-type protein or of the HgS_3 model compound, although still within the range for 3 coordinate Hg−S centers. Thus, perhaps a third sulfur ligand to Hg in this protein is contributed by a buffer thiol yielding a tricoordinate structure perturbed somewhat in its geometry compared to the wild-type protein, possibly by the bulk of the adjacent tyrosine. Note that HPLC-ESI-MS observations (above) indicated that C126Y binds three BME molecules under conditions in which it also binds Hg.

Hg(II) Binding. In early work, the wild-type MerR proteins of Tn*501* (*15*) and of Tn*21* (*13*) were found to have half-saturation concentrations for Hg(II) of 10^{-7} M in the presence of millimolar buffer thiols. These measurements were carried out by gel filtration and resulted in simultaneously diluting both the protein and the Hg(II) (although maintaining a constant thiol concentration). Shewchuk et al. found that at concentrations below 1 μM the protein dissociated into monomers and bound Hg(II) less well. As noted above (Figure 3AB), using a different buffer system, we found that full-length MerR and the most extensively deleted variant did not appreciably dissociate into monomers in the 1−5 μM range and, thus, we used concentrations in this range to assess the binding properties of these proteins. We used two methods to measure the Hg(II) affinity of MerR and its derivatives: equilibrium dialysis using ultrafiltration (Figure 5) and nonequilibrium dialysis (Table 2).

Equilibrium ultrafiltration showed that even the most extensively deleted variant ($\Delta\Delta$; Figure 5A) was considerably more effective in binding Hg(II) than was the missense mutant C126Y and was only slightly less avid for Hg(II) than the full-length protein. The three N-terminal deletion mutants also exhibited affinity for Hg(II) similar to that of the full-length protein (Figure 5B), and two of them (Δ47 and Δ65) consistently bound more Hg(II) than the full-length protein. The variances in these data precluded the derivation of reliable dissociation constants by Scatchard analysis for any but the full-length protein for which a K_d of 0.4 μM and a Hg(II)/$MerR_2$ ratio of 1.1 were calculated (*44*). However, all of the deletion variants saturate considerably closer to the Hg(II)/$MerR_2$ ratio of the full-length protein than they do to that of the C126Y missense mutant.

In nonequilibrium dialysis, loss of Hg(II) from each protein (corrected for free diffusion of the ion) exhibits first-order exponential behavior (data not shown) and reveals clear functional distinctions among them (Table 2). The two less extensive N-terminal deletion derivatives (Δ47 and Δ65) are very similar to the full-length protein in their off rates for Hg(II) and their extrapolated stoichiometry. In contrast, both the longest N-terminal deletion (Δ79) and the double deletion derivative ($\Delta\Delta$) lose Hg(II) from 4- to 5-fold faster than the full-length protein, although their extrapolated stoichiometry is no less than that of the full-length protein. However, as seen by equilibrium ultrafiltration none of the deletion derivatives is as impaired in its affinity for Hg(II) as is C126Y which loses Hg(II) nearly 9-fold faster than the full-length protein and similarly has a low Hg(II)-$MerR_2$ stoichiometry.

DISCUSSION

Our observations indicate that removal of just the DNA binding domain of MerR or even of the two predicted immediately distal helical domains does not eliminate the ability of the remaining residues to bind Hg(II) with high affinity. We find that residues from C80 through C128 of MerR are sufficient to form a Hg(II)-binding domain with a capability of competing with low molecular weight thiols for binding Hg(II) comparable to that of the full-length protein. While the precise mechanistic basis for this phenomenon remains to be determined, data presented here suggest that it resides to some degree in the ability of these residues (which comprise only about one-third of this relatively small protein) to form stable dimers (Figure 3).

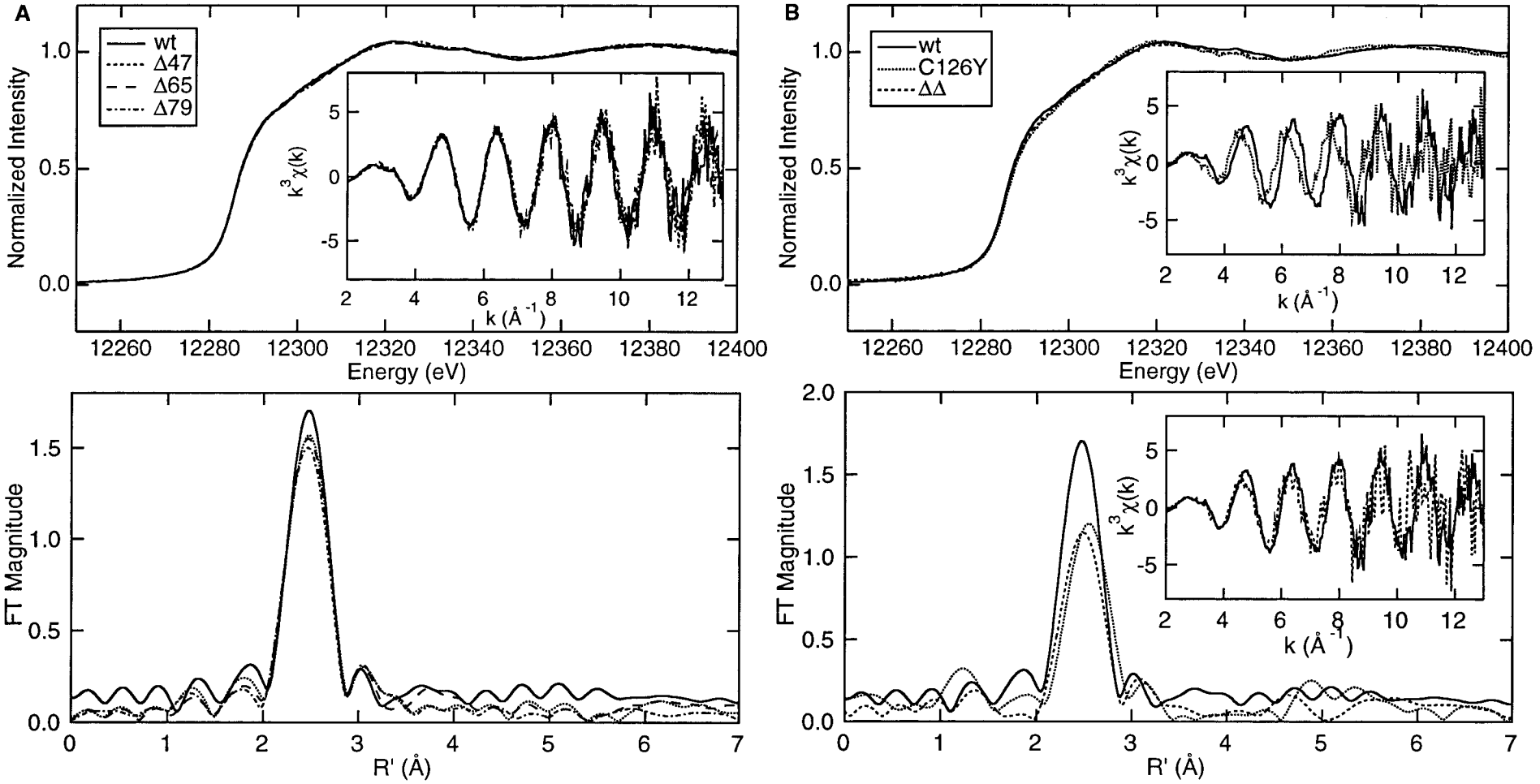

FIGURE 4: X-ray spectroscopy of the Hg(II) complexes with MerR variants. XAS edge and EXAFS spectra (upper graph and its insert, respectively) and EXAFS Fourier transform (lower graph) comparison of (A) full-length wild-type MerR and the three least extensive N-terminal deletion derivatives; and (B) the full-length wild-type MerR, the missense mutant C126Y, and the most extensively deleted mutant, ΔΔ. Inserts: (upper portion), EXAFS comparison of wild-type and C126Y; (lower portion), EXAFS comparison of wild-type and ΔΔ mutant. Symbols designate samples as indicated in each section. Conditions are given in Table 1.

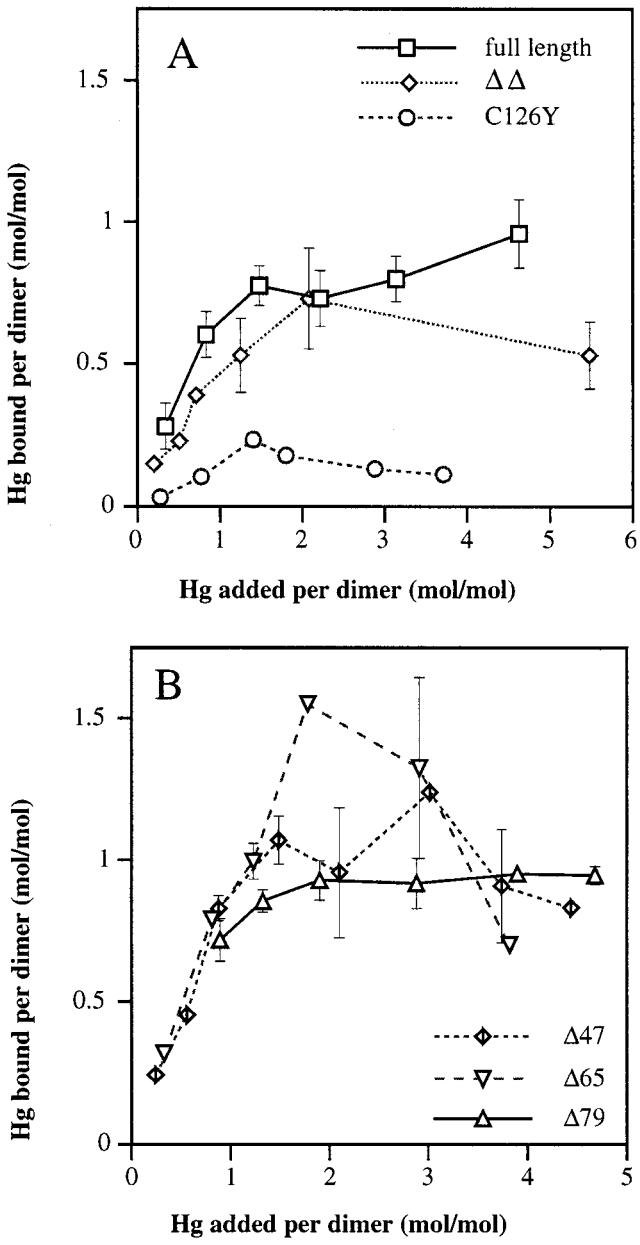

FIGURE 5: Equilibrium ultrafiltration determination of the Hg(II) binding properties of MerR and its mutant derivatives. Hg(II) bound per dimer as a function of added Hg(II) for (A) full length wild-type MerR (open squares), deletion mutant ΔΔ (open diamonds), and missense mutant C126Y (open circles); and (B) N-terminal deletion mutants Δ47 (slashed diamond), Δ65 (open inverted triangles), and Δ79 (open triangles). Protein concentrations were either 1 or 2 μM. Data points are the averages of at least two trials (± standard error) for each protein except C126Y.

Work with model 3-helix-bundle oligopeptides designed to assemble trigonal Hg-binding domains (*24*, *25*) is instructive in this context. At concentrations so dilute that a low MW thiol would not form a stable tricoordinate complex with Hg(II), the monocysteine derivative of the helix bundle-forming peptide Tri readily forms a trimer structure with an HgS_3 center. The effect of varying the position of the cysteine within the peptide clearly implicated helix packing in forming this stable three-coordinate metal binding site. Unlike these artificial peptides MerR provides two thiol ligands (C117 and C126) to Hg from one chain and the third ligand (C82) from the other chain of a dimeric quaternary structure (*17*, *27*). However, our data suggest that MerR may have more in common with such synthetic helix bundle proteins than was previously realized. The region between C82 and C117 of MerR is strongly predicted to form an α-helix and between residues 82 and 112 to form either a parallel or antiparallel dimeric or trimeric coiled-coil structure similar to that of the designed Hg-binding helix bundle oligopeptides. Our CD observations indicate that the region certainly has a stable α-helical character. The implications of each of these potential structures for the formation of Hg(II)-binding sites in MerR is outlined in Figure 6.

Table 2: Rate of Hg(II) Loss by MerR and Its Variants

protein	k_{off} (nmol of Hg(II)/h per μmol dimer)[a]	binding sites/dimer
full length	17	0.73
Δ47	7	0.81
Δ65	14	0.82
Δ79	78	1.54
ΔΔ	90	1.20
C126Y	152	0.26

[a] k_{off} was measured by nonequilibrium dialysis on 10 μM protein at 4 °C and is corrected for free diffusion of Hg(II). See details in Experimental Procedures. All conditions were tested on at least two occasions for all proteins. R^2 range: 0.72−0.95.

The prediction of a relatively rigid α-helix between residues 82 and 117 and genetic data for an intersubunit Hg(II) binding site involving C82 from one subunit and C117 and C126 from the other lead to two models for this region involving an antiparallel arrangement of either a standard α-helix with 7.2 residues per 2 turns (Figure 6A, upper section) or a coiled-coil heptad-repeat helix with 7.0 residues per 2 turns (Figure 6A, lower section). In the standard α-helical structure, C82 and C117 would lie nearly on opposite faces of the helix which, depending on other constraints on this region, could lead to there being only a single site available at one end of the antiparallel paired helices. However, helix rotation or mobility at the ends of the helices could result in sufficient proximity of the thiols at each end of the structure to allow formation of an Hg(II)-binding site at each end of the dimeric structure. In the coiled-coil model, which has a shorter helix repeat, both C82 and C117 would be in the "a" (or "1") position of the heptad repeat; i.e., they would be in equivalent positions with respect to the helix axis, and therefore would lie on the same face of the helix. In this arrangment it would seem that equivalent Hg(II)-binding sites could quite readily form at each end of the coiled-coil. Indeed, it may be the case that in the dimeric apoprotein two symmetrical high affinity Hg(II)-binding sites do exist, but as soon as one potential site binds Hg(II), the resulting allosteric change (ref *8*; and R. Kulkarni and A. O. Summers, submitted for publication) renders the other potential high affinity site nonfunctional, i.e., unable to compete effectively with buffer thiols for Hg(II).

In this light, it is noteworthy that by both measures of Hg(II) affinity (Table 2 and Figure 5) the intermediate length derivatives (Δ47, Δ65, and Δ79) bind more Hg(II) per dimer than the full-length wild-type protein, suggesting that they might actually form two high affinity sites. The Hg(II) off-rates for the first two of these derivatives are also less than or equal to those of the full-length protein, suggesting that their Hg(II)-binding sites are reasonably stable even with millimolar competing thiol. However, we must also consider

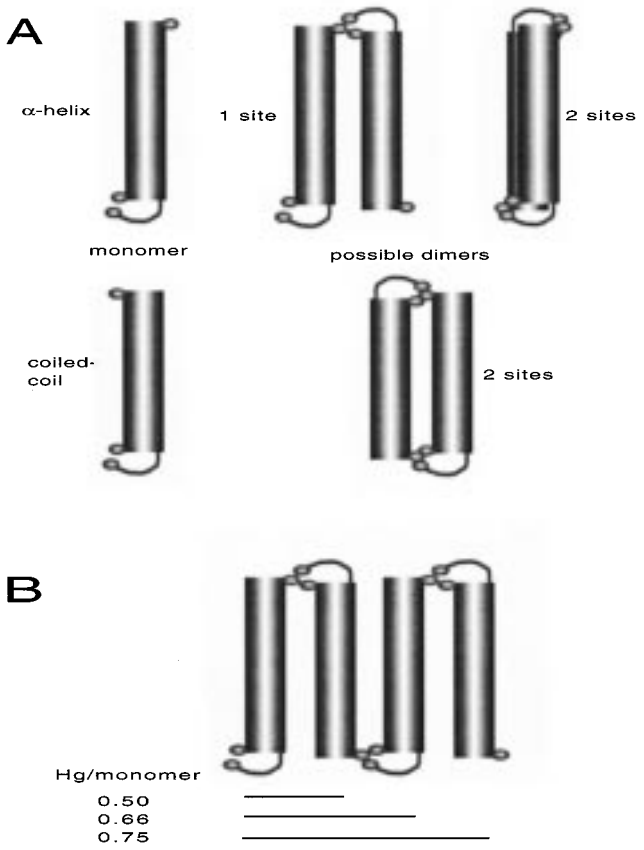

FIGURE 6: Alternative models for the role of the C82−C117 helical domain in MerR dimerization and formation of the Hg(II) binding site. Tube = helical region. The putative loop between C117 and C126 is indicated by a curved line. Spheres = thiol groups on cysteines 82, 117, and 126. (A) Upper section: monomer and possible Hg(II)-binding dimer structures of this region in a standard α-helical conformation (3.6 residues per turn); lower section: monomer and possible Hg(II)-binding dimer structure of this region in a coiled-coil conformation (3.5 residues per turn). (B) Possible effect of multimerization on the apparent Hg(II)-MerR stoichiometry; monomers depicted are of the standard α-helical conformation; however, we do not preclude formation of analogous higher order aggregates by a coiled-coil conformation of MerR.

that the apparently higher Hg(II)/protein stoichiometry could simply be an artifact of multimerization, since antiparallel trimers or tetramers might contribute to metal binding in ways which would increase the mass of Hg(II) bound per mass of protein (Figure 6B). We observed multimerization in gel filtration in experiments designed only to ask whether MerR and one of its deletion derivatives could form stable dimers in the absence of added Hg(II) and under rigorous anaerobic conditions. In earlier work, Shewchuk et al. (*15*) used aerobic gel filtration to assess the Hg(II)-binding stoichiometry of wild-type MerR and did not report multimerization. Future work will determine whether Hg(II)-binding influences multimerization of MerR and its deletion derivatives.

Previous biochemical observations (*15*) are also consistent with the model(s) for MerR structure proposed here. Shewchuk et al. found that DTNB catalyzed a disulfide exchange resulting in a MerR disulfide dimer, suggesting that at least one cysteine on each monomer is close to the dimer interface. They also found that the C82Y or C82A proteins were less likely to form intersubunit disulfide dimers than the wild-type or any substitutions at positions 115, 117, or 126. All eight cysteines per dimer reacted with *p*-hydroxy-mercuri-benzoate but only six cysteines per dimer reacted with dithionitrobenzoic acid or iodoacetamide even in 6 M guanidine. The authors concluded that all of the cysteines were in the thiol form, but that two per dimer must be kinetically inaccessible to DTNB; our ESI-MS observations are consistent with the idea that only three thiols per monomer are available to form disulfides with BME. Upon addition of Hg(II), Shewchuk et al. (*15*) found two cysteines per dimer were protected from DTNB and iodoacetylated tryptic peptides revealed that this was C117. Hg(II) did not alter the iodoacetylation of C115 or C126 and C82 was unreactive to iodacetamide with or without Hg(II). Surprisingly, proteolytic removal of the C-terminus from approximately residue 120 or 121 (*15*) resulted in an N-terminal protein fragment that dimerized and bound DNA, but not Hg(II), thus implicating C126 in Hg(II)-binding despite the apparent lack of effect of Hg(II)-binding on iodoacetylation at that residue. Assuming a simple 2-fold (parallel) C_2 symmetry of the dimer, the authors concluded from these observations that C82 was near the dimer interface but had no role in Hg(II) binding and that C117 and C126 were the sole ligands to Hg(II) in either a two- or four-coordinate arrangement. This conclusion was limited by the fact that the C82s were "invisible" to iodoacetamide and so their relationship to Hg(II) could not have been reported by this reagent. Our data indicating a long α-helix between C82 and C117 rules out parallel C_2 symmetry as a means of effecting the requisite propinquity of the three metal ligands, however, C82 is also central to the formation of disulfide cross-linked dimers in both models offered here. In both antiparallel models C82 could form a disulfide with either C117 or C126 on the other monomer and if either C117 or C126 were missing the remaining one on the same monomer would be available to interact with C82 on the other monomer. The failure of C126 to be protected by Hg(II) from iodoacetylation (*15*) remains difficult to explain in either a parallel or antiparallel model, unless the putative allosteric change induced by Hg(II) also affects the reactivity of the remaining cysteines to other electrophilic reagents as well as to Hg(II).

Unusual reactivity in cysteines is often the rule in proteins involved in redox reactions (*45*), and it has received particular attention recently in two members of the thioredoxin superfamily: glutaredoxin and DsbA. In each of these proteins, a cysteine has a very low pK_a (*46*, *47*) and two independent models are offered for the stabilization of the thiolate anion. Using a model peptide system, Kortemme and Creighton (*46*) demonstrated that a thiolate at such positions can be stabilized by favorable interactions with the helix dipole. In MerR, although C82 lies at the N-terminus of a predicted long α-helix, the helix macrodipole would likely cancel in the postulated antiparallel dimer configuration, suggesting that local electrostatic interactions might be more significant in modulating cysteine reactivity. In this respect it is noteworthy that Grauschopf et al. (*47*) demonstrated that alteration of the two residues between the cysteines in the CPHC active site of DsbA profoundly affected the redox potential of this protein. A possible role for the adjacent histidine in stabilizing a thiolate at C30 of DsbA was suggested by electrostatic calculations. Although MerR has no CXXC motifs, there are conserved histidine residues near C82 and C117 (H81 and H118, respectively). We are

exploring the relevance of these observations to full-length MerR and the deletion variants described here, as a thiolate with a very low pK_a is also expected to be less reactive (*45*, *48*).

Our observations suggest that metal recognition by MerR is largely embodied in a discrete domain consisting of only one-third of the protein. Moreover, this domain also functions as a component of the dimer interface of the protein, likely assuming an antiparallel helix bundle or coiled-coil structure. The ability of MerR to bind but a single Hg(II) per dimer despite having two potential binding sites is retained by extensively shortened derivatives offering promise that the mechanistic basis of this apparent paradox and of metal specificity itself can be resolved in these simpler model proteins. Nonetheless, it is important to note that to date all studies of Hg(II) binding by full-length MerR have only measured this property when the protein was not bound to DNA (ref *17*, and above), when DNA was added to a preformed Hg(II)-MerR_2 complex (*26*), or when only 1 equiv of Hg(II) per dimer was provided to DNA-bound MerR (*15*). Thus, the stoichiometry of the MerR−Hg(II) interaction may be different when examined with the other components of the actual preinitiation complex, DNA, and/or RNA polymerase.

ACKNOWLEDGMENT

We thank Dennis Philips for HPLC-ESI-MS analysis, Jon Amster and Michelle Trester for ESI-MS analysis, Mike Johnson for assistance with CD experiments, Tracy Smith and Keith Pitts for mercury analysis, and Jon Caguiat for resistance phenotype determination. We also thank Tom O′Halloran, Jim Penner-Hahn, Him-Tai Tsang, and Steve Watton for published and unpublished XAS data on Tn*501* MerR-Hg(II) and various Hg(II) model compounds. We are grateful for thoughtful criticism of the manuscript by Jon Caguiat, Harry Dailey, Tim Hoover, Resham Kulkarni, Heather Lumppio, and Ellen Neidle.

REFERENCES

1. Misra, T. K. (1992) *Plasmid 27*, 4−16.
2. Summers, A. O. (1992) *J. Bacteriol. 174*, 3097−3101.
3. Heltzel, A., Lee, I. W., Totis, P. A., and Summers, A. O. (1990) *Biochemistry 29*, 9572−9584.
4. Lee, I. W., Livrelli, V., Park, S.-J., Totis, P. A., and Summers, A. O. (1993) *J. Biol. Chem. 268*, 2632−2639.
5. Livrelli, V., Lee, I. W., and Summers, A. O. (1993) *J. Biol. Chem. 268*, 2623−2631.
6. Cowell, I. G. (1994) *Trends Biochem. Sci. 19*, 38−42.
7. Fondell, J. D., Roy, A. L., and Roeder, R. G. (1994) *Genes Dev. 7*, 1400−1410.
8. Helmann, J. D. (1997) in *Metal Ions in Gene Regulation* (Walden, W. E., and Silver, S., Eds.) pp 45−76, Chapman & Hall, London.
9. Ansari, A. Z., Chael, M. L., and O'Halloran, T. V. (1991) *Nature 355*, 87−89.
10. Condee, C. W., and Summers, A. O. (1992) *J. Bacteriol. 174*, 8094−8101.
11. Ansari, A. Z., Bradner, J. E., and O'Halloran, T. V. (1995) *Nature 374*, 371−375.
12. Ross, W., Shore, S. H., and Howe, M. M. (1986) *J. Bacteriol. 167*, 905−919.
13. Shewchuk, L. M., Helmann, J. D., Ross, W., Park, S. J., Summers, A. O., and Walsh, C. T. (1989) *Biochemistry 28*, 2340−2344.
14. Shewchuk, L. M., Verdine, G. L., Nash, H., and Walsh, C. T. (1989) *Biochemistry 28*, 6140−6145.
15. Shewchuk, L. M., Verdine, G. L., and Walsh, C. T. (1989) *Biochemistry 28*, 2331−2339.
16. Helmann, J. D., Wang, Y., Mahler, I., and Walsh, C. T. (1989) *J. Bacteriol. 171*, 222−229.
17. Helmann, J. D., Ballard, B. T., and Walsh, C. T. (1990) *Science 247*, 946−948.
18. Comess, K. M., Shewchuk, L. M., Ivanetich, K., and Walsh, C. T. (1994) *Biochemistry 33*, 4175−4186.
19. Wright, J. G., Natan, M. J., MacDonnell, F. M., Ralston, D. M., and O'Halloran, T. V. (1990) in *Progress in Inorganic Chemistry*, (Lippard, S. J., Ed.) Vol. 38, pp 323−412, Wiley-Interscience, New York.
20. Wright, J. G., Tsang, H.-T., Penner-Hahn, J. E., and O'Halloran, T. V. (1990) *J. Am. Chem. Soc. 112*, 2434−2435.
21. Utschig, L. M., Wright, J. G., and O'Halloran, T. V. (1993) *Methods Enzymol. 226*, 71−97.
22. Wright, J. G. (1991) pp 330, Northwestern University, Evanston, Illinois.
23. Ralston, D. M., and O'Halloran, T. V. (1990) *Proc. Natl. Acad. Sci. U.S.A. 87*, 3846−3850.
24. Dieckmann, G. R., McRorie, D. K., Tierney, D. L., Utschig, L. M., Singer, C. P., Ohalloran, T. V., PennerHahn, J. E., DeGrado, W. F., and Pecoraro, V. L. (1997) *J. Am. Chem. Soc. 119*, 6195−6196.
25. Dieckmann, G. R., McRorie, D. K., Lear, J. D., Sharp, K. A., DeGrado, W. F., and Pecoraro, V. L. (1998) *J. Mol. Biol. 280*, 897−912.
26. Utschig, L. M., Bryson, J. W., and O'Halloran, T. V. (1995) *Science 268*, 380−385.
27. Ross, W., Park, S.-J., and Summers, A. O. (1989) *J. Bacteriol. 171*, 4009−4018.
28. Barrineau, P., and Summers, A. O. (1983) *Gene 25*, 209−221.
29. Zeng, Q., Eidsness, M. K., and Summers, A. O. (1997) *BioTech 23*, 412−418.
30. Gill, S. C., and Von Hippel, P. H. (1989) *Anal. Biochem. 182*, 319−326.
31. Heltzel, A., Gambill, D., Jackson, W. J., Totis, P. A., and Summers, A. O. (1987) *J. Bacteriol. 169*, 3379−3384.
32. Sun, H. Y., and Wang, K. (1995) *J. Inorg. Biochem. 60*, 79−87.
33. Mehta, P. K., Heringa, J., and Argos, P. (1995) *Protein Sci. 4*, 2517−2525.
34. Rost, B. (1994) *Comput. Appl. Biosci. 10*, 53−60.
35. Brennan, R. G., and Matthews, B. W. (1989) *J. Biol. Chem. 264*, 1903−1906.
36. Wolf, E., Kim, P. S., and Berger, B. (1997) *Protein Sci. 6*, 1179−1189.
37. Lupas, A. (1997) *Curr. Opin. Struct. Biol. 7*, 388−393.
38. Christie, G. E., White, T. J., and Goodwin, T. S. (1994) *Gene 146*, 131−132.
39. Rensing, C., Mitra, B., and Rosen, B. P. (1997) *Proc. Natl. Acad. Sci. U.S.A. 94*, 14326−14331.
40. Osborn, A. M., Bruce, K. D., Strike, P., and Ritchie, D. A. (1995) *Syst. Appl. Microbiol. 18*, 1−6.
41. Nucifora, G., Chu, L., Silver, S., and Misra, T. (1989) *J. Bacteriol. 171*, 4241−4247.
42. Barrineau, P., Gilbert, M. P., Jackson, W. J., Jones, C. S., Summers, A. O., and Wisdom, S. (1984) *J. Mol. Appl. Genet. 2*, 601−619.
43. Fairman, R., Chao, H.-G., Mueller, L., Lavoie, T. B., Shen, L., Novotny, J., and Matsueda, G. R. (1995) *Protein Sci. 4*, 1457−1469.
44. Clarke, A. R. (1996) in *Enzymology* (Engel, P. C., Ed.) pp 199−220, BIOS Scientific Publishers, Ltd., Oxford, UK.
45. Gilbert, H. F. (1990) *Adv. Enzymol. 63*, 69−172.
46. Kortemme, T., and Creighton, T. E. (1995) *J. Mol. Biol. 253*, 799−812.
47. Grauschopf, U., Winther, J. R., Korber, P., Zander, T., Dallinger, P., and Bardwell, J. C. A. (1995) *Cell 83*, 947−955.
48. Szajewski, R. P., and Whitesides, G. M. (1980) *J. Am. Chem. Soc. 102*, 2011−2025.

BI9817562